A flight performance based optimization model for eVTOL vehicles

Nikhilesh Tumuluru Ramesh*
University of Waterloo, Waterloo, Canada

Pradeep V. Pandurangi†
Mumbai, India

The need for sustainable transportation and expanding urbanization has provided a strong impetus for the development of eVTOL (electric Vertical Take-Off and Landing) aircraft in recent years. Although the first generation of such aircraft may enter the skies over the next couple of years, there is great variety in designs, and no consensus on one optimal configuration yet. In the present study, a flight performance based optimization model is proposed for aircraft sizing of a typical electric tilt-rotor. A constrained genetic algorithm is used with the objective function of gross weight minimization. The adoption of key aircraft performance parameters such as the turning radius and climb rate into the model, in addition to traditional design parameters are found to be important drivers of the optimization. The optimization is run for varying payloads (300, 500 and 700 kg) and ranges (50, 150 and 200 km) to gain insights into the scalability of aircraft and component designs. The wing and motors, both of which contribute significantly to the overall empty weight, are found to drive the optimization in different directions, with the program subsequently attempting to find an optimal solution.

Nomenclature

DEP	=	Distributed Electric Propulsion
UAM	=	Urban Air Mobility
RAM	=	Regional Air Mobility
$VTOL$	=	Vertical Take-Off and Landing
$eVTOL$	=	Electric Vertical Take-Off and Landing
W/S	=	Wing Loading in N/m^2
b	=	Wingspan in m
U_{cr}	=	Cruise speed in m/s

*PhD Candidate, Mechanical and Mechatronics Engineering, University of Waterloo
†

D = Propeller Diameter in m

AR = Main Wing Aspect Ratio

C_D = Coefficient of drag

C_f = Skin friction drag

FF = Form factor

C_{D0} = Zero lift drag

S_{wet} = Wetted surface area in m^2

Re = Reylond's number

C_{ft} = Skin friction drag for trubulent flow

M = Mach number

t/c = thickness to chord ratio

x_t = the position of maximum thickness on the airfoil

e = Oswald factor

BEM = Blade Element Momentum

T/W = Thrust to weight ratio

q = Dynamic pressure in kg/ms^2

C_{Dmin} = Minimum drag coefficient

k = Lift induced drag constant

ϕ = Bank angle in radians

V_v = Vertical velocity in m/s

n = Load factor

GW = Gross weight in kg

L/D = Lift to drag ratio

I. Introduction

The drive towards greater overall sustainability has promoted the development of many new technologies. Pertinent to the aviation and automotive industry, the use of electricity as the primary power source is increasingly supplanting conventional fossil fuels. While electric cars are rapidly proliferating the markets, electric aviation is in a relatively nascent stage. Currently, the developments in battery technology have made it feasible to design eVTOL aircraft capable of carrying payloads up to 800 kg for short to medium distance (30-800 km) trips [1]. Electric propulsion engenders multiple benefits when compared with gasoline engines. In particular, unlike gasoline engines, electric motors are efficient at various sizes, allowing for Distributed Electric Propulsion (DEP) systems consisting of multiple

motors. Furthermore, the decreased complexity in auxiliary components required for electric motors enables design of comparably light aircraft capable of vertical take off and landing (VTOL). Additionally, the reduction in noise achievable through the use of electric propulsion [2] have made eVTOL's attractive as a mode of transportation within urban areas (Urban Air Mobility) as well as nearby cities (Regional Air Mobility).

The flexibility introduced by VTOL and DEP capabilities have led to a large number of unconventional design configurations for these aircraft. Most popular among the designs include lift + cruise, tilt rotor, tilt wing, multirotor, or a hybrid combination of these, among others [3]. Many studies have explored the various design and feasibility aspects for each of the different configurations. Bachinni and Cestino [3] discuss the advantages and limitations of different eVTOL concepts. They make a preliminary comparison of energy requirements of three different configurations- multirotor, lift+cruise and the ducted tilt wing, and conclude that each is suited for different mission range. Specifically, the multirotor system is typically more efficient for short trips, and the ducted tilt wing for long distances. Nathan et al. [4] perform a rigorous first order technical feasibility analysis of the ducted vectored tilt wing configuration. They calculate the energy requirements for battery sizing by considering the energy consumption during different phases of flight and energy requirements of the auxillary components. Additionally, a preliminary noise assessment for the ducted rotor concept is provided. A number of other studies (e.g. [5–7]) have been conducted to asses the technological feasibility and/or to propose conceptual designs for different eVTOL configurations. Similar to conventional aircraft design, where fuel efficiency is an important driving factor for any proposed design, the objective of many eVTOL conceptual designs is to minimize energy consumption for a desired mission while trying to maximize the range and payload capabilities within the bounds of other constraints. The design flexibility offered by eVTOL vehicles allows for the tuning of a vast array of design and performance parameters for a given payload and range in order to arrive at a feasible configuration design. Key design parameters considered by many studies include, but are not limited to: wing loading (W/S), disc loading, wingspan or footprint (b) , number of rotors, cruise speed (U_{cr}), empty weight fraction, rotor tip speed, rotor diameter (D), lift to drag ratio (L/D), and wing aspect ratio (AR). The choice of these parameters is in turn driven by mission requirements, where for example a design driven by noise reduction might focus on lower rotor tip speeds.

Many studies have focused on design optimization by considering different objective functions (cost/gross weight/noise or some combination of the these) through exploration of design parameter spaces. Kadiresan and Duffy [8] employed a weights based optimization to compare the gross weight of five different eVTOL configurations. They considered a simplified mission profile, and omitted noise and cost metrics from their optimization. Additionally, they considered a fixed footprint of 50 feet and performed the optimization for sweeps of wing loading and propeller diameters. Their results show the optimal configurations for different ranges and speeds. Similar to [3], multirotors which are efficient in hover due to their low disc loading, are more suited for small distances, while concepts that

involve tilting mechanisms (wing/rotor) are efficient in long distances with lift+cruise concepts falling in between the two extremes. Brown and Harris [2] used geometric programming optimization to perform a trade off study for nine different vehicle configurations. Specific importance was given to noise generated, and cost of operation was also considered. A New York city route is also used as a reference mission. Their results show that urban air mobility is economically viable compared to existing helicopter routes with substantial potential for noise reduction. Configurations with higher lift to drag ratios and higher disc loading were found to cost less at the expense of increased noise. Lee et. al. [9] performed an optimization study for the conceptual design of an eVTOL Personal Air Vehicle (PAV) using design of experiments. For their models, data provided from Uber and Vahana were used as input while setting the gross weight, power to weight ratio, footprint, and the lift to drag ratio as the design target parameters.

The different studies discussed generally perform a preliminary sizing of the battery, and ultimately, the aircraft through the use of the various design parameters. However, the interdependencies amongst the different parameters and their combined effect on the gross weight through the use of first principles have not been discussed in detail. Specifically, in the conceptual design stage of an aircraft, it is typical to prescribe desired performance parameters that conform to the flight envelope such as required radius of turning and climb rate. In order to meet the desired aircraft performance requirements, there are relationships between some design parameters that must be satisfied, such as through the use of a constraint diagram [10]. Defining these aircraft performance parameters in addition to conventional parameters like the payload, range, cruise velocity, wing loading e.t.c, serves a dual purpose. First, it helps to arrive at a more holistic conceptual design that considers a broader scope of design and performance parameters, thereby decreasing the likelihood of complete design overhauls through the subsequent preliminary and detailed design phases. Secondly, and more importantly, it helps to provide a framework based on first principles that can be used to arrive at more optimized design configurations. In the present work, a weights based optimization using a genetic algorithm is performed while enforcing performance parameters (constant velocity banking and climb rate) in addition to four design parameters (Wing Loading, Rotor diameter, Rotor RPM, and Cruise speed). The objective of the work is to introduce an alternative approach to the design optimization of eVTOL's in general, and only a single configuration (tilt rotor) is chosen as the reference configuration. However, the model itself is independent of the chosen configuration, and can be applied to other configurations with minimal modifications. Moreover, cost and noise are not considered here, but can also be incorporated with appropriate modifications.

II. Mission and Vehicle Assumptions

A typical eVTOL configuration is selected for optimization in this paper: a tilt-rotor with six rotors, four on the main wing and two on the horizontal tail as shown in figure 1 with further details in table 1. Each rotor is assumed to have three-bladed propeller. Since the objective is to size the aircraft for various payloads, CAD models of 3,5 and 7 seater

aircraft (corresponding to 300, 500 and 700 kg payloads) were created in OpenVSP to serve as inputs for the geometrical constraints of the fuselage and rotor placements. The payload and range (50, 150 or 250 km) serve as input parameters whereas the cruise speed, wing loading, rotor diameter and rotor RPM at cruise are the key variables being optimized, which will be further elaborated in the next section. In this section, the mission and vehicle assumptions are presented.

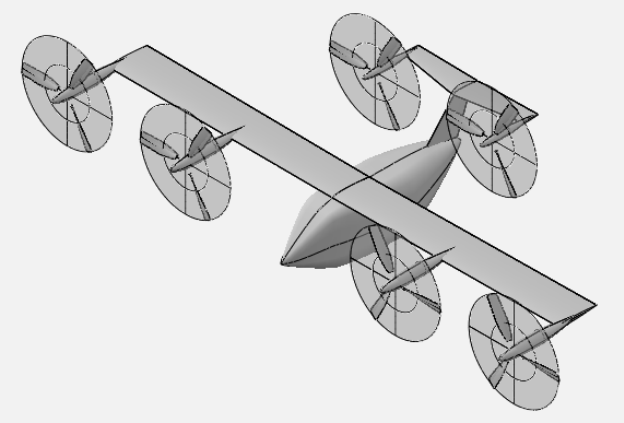

Fig. 1 Tilt rotor configuration with 6 rotors.

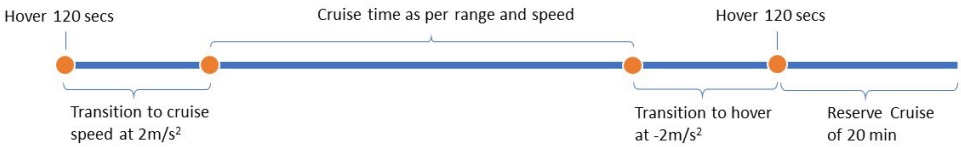

Fig. 2 Mission Diagram.

Depending on the range selected, the aircraft is optimized for either a UAM mission which is typically less than 100 km or RAM mission which is typically greater than 200 km, however the cruise altitude assumed in both cases is 1,000 m. The complete mission profile is shown in figure 2, and key assumptions are tabulated in table 2. A reserve cruise of 20 minutes is factored into the design during energy consumption analysis. The reserve requirements will be driven primarily by the regulations being created for electric aircraft by various certification authorities. Whether these will be adopted from existing general aviation regulations or revised to suit electric aircraft operation remains to be seen. Here it is pertinent to mention the high level of safety offered by the inherent redundancy of DEP. The present study takes into account a motor-out condition, where in the case of failure of one of the motors, the corresponding motor on other wing is shut off and aircraft is able to maintain full flight authority with only four of the six motors functioning.

Battery pack energy density is one of the key assumptions in eVTOL design. While several presently available battery chemistry and their performance were evaluated, it is not within the scope of this paper to compare and choose the optimal solution. A sufficiently high pack level battery energy density of 300 Wh/kg was chosen. This battery density

Table 1 Vehicle Assumptions

Parameter	Assumption
Aircraft configuration	Tilt-rotor
Number of rotors	6
Number of propeller blades/rotor	3
Main Wing AR	12

Table 2 Mission Assumptions

Parameter	Assumption
Cruise Altitude	1,000 m
Take-off hover	120 s
Landing hover	120 s
Transition from hover to cruise	2 m/s^2
Transition from cruise to hover	-2 m/s^2
Reserve Cruise	20 min

Table 3 Powertrain Assumptions

Parameter	Assumption
Battery Pack Density	300 Wh/kg
Battery Reserve	20%
Powertrain Efficiency	75%

performance is expected to be reached by 2026 [11]. Furthermore, it is assumed that the battery specific power is sufficient for take-off, and landing at minimum battery voltage condition (e.g. after a 20 minute reserve cruise flight following a balked landing scenario). The battery cycle life is a variable that would affect the economic viability of the aircraft rather than the technical feasibility and hence it is not included in the analysis. 20% of the battery energy is considered unusable in accounting for the safety reserve and environmental as well as temporal degradation. The battery volumetric density is not considered a key constraint at this stage of configuration selection, since sub-system packaging is not part of the optimization. It is assumed that the energy consumed by auxiliaries will be minimal and is not added to the energy calculations. Battery operation at nominal temperatures is assumed and no further knockdown or safety factors considered for temperature related fluctuations in energy density. Overall powertrain efficiency of 75% is considered to account for the wiring, motor controller, motor and propeller efficiencies.

A. Weight Model

The empty weight estimations for eVTOLs is challenging due to lack of historical data and novelty of each concept. However, historical data of similarly sized general aviation aircraft can be used to estimate the structural weight. The

electric powertrain weights are estimated using references that have benchmarked available electric motors, controllers and propellers. Accessories and furnishing weights are assumed to be similar to existing general aviation aircraft.

The airframe empty weight estimates are based on empirical formulas for general aviation aircraft presented by Raymer [12]. The fuselage dimensions for each payload capacity are estimated by creating CAD models on OpenVSP and adding the appropriate number of seats, considerations for luggage compartment and approximate tail location. For the 300 kg payload, fuselage is sized for seating capacity for three people (1 pilot + 2 passengers). Similarly, the 500 kg payload considers five seats, and the 700 kg variant has seven seats. The fuselage lengths are 4.5 m, 6 m and 7 m respectively. The current formula requires lengths from front bulkhead to aft frame, since the section in front and rear of these frames are to be short and the fuselage lengths themselves are used as inputs. The fuselage cross-section is kept constant considering a rounded rectangle cross-section with height of 1.7 m and width of 1.5 m. The wetted area and tail arm length of each of the fuselages is also derived for the CAD models. The fuselage is unpressurised since cruise altitude is only 1,000 m.

For the wing weight, a rectangular wing is considered that does not consider bending moment relief due to motors and/or batteries installed in the wings. The ultimate load factor is 4.5, considering a maximum positive load factor of 3 at cruise velocity and 1.5 as safety factor. The thickness to chord ratio is assumed to be 0.14 for the main wing. The horizontal and vertical tail areas are sized as per the methodology described in Gudmundsson [10] with AR of 6 and 2 respectively considering zero sweep angle and t/c ratio of 0.14. A tricycle arrangement is considered for the landing gear with a length of 0.6 m for both the main and nose landing gear, and a value of 2.5 is assumed for ultimate landing load factor. This type of landing gear will allow the aircraft to glide and land in case of powertrain or tilt mechanism failure

The electric motor, motor controller, propeller and hub weights are estimated using formulae presented in the paper by Kadhiresan et al. [8]. Furthermore, the weight of additional equipment, furnishings, etc. are estimated from Smart et al. [13]. The final empty weight estimate of the configuration is found by adding up all the component weights mentioned in Appendix A.

B. Drag Model

The zero lift drag of the aircraft is calculated by using a component build up model. Several key contributors to drag are considered: fuselage, wing, tail assembly, motor pods, landing gears, induced drag and miscellaneous drag caused by air leakage and protruding geometries.

For each of the components (except the miscellaneous drag) the zero lift drag derives from combining the skin

friction drag C_f, a form factor FF to account for the pressure drag, and an interference factor Q as follows:

$$C_{D0} = \sum_{0}^{n} C_f * FF * Q * \frac{S_{wet}}{S_{ref}} \tag{1}$$

Here, the summation is carried out over the number of components considered, with S_{wet}/S_{ref} being the ratio of component wetted area to a reference area (taken here as the wing area).

The skin friction drag for laminar flow is calculated as:

$$C_{fl} = \frac{1.328}{\sqrt{Re}} \tag{2}$$

where Re is the Reynolds number. The skin friction drag for turbulent flow is calculated as:

$$C_{ft} = \frac{0.455}{(logRe)^{2.58}(1 + 0.144M^2)^{0.65}} \tag{3}$$

where M is the Mach number. To account for combined turbulent and laminar flow, the resultant skin friction drag is calculated as:

$$C_f = pC_{fl} + (1 - p)C_{ft} \tag{4}$$

with p representing the percentage of the component exposed to laminar flow. The form factor for the wing is calculated as:

$$FF_w = [1 + (0.6/x_t)(t/c) + 100(t/c)^4][1.34M^{0.18}] \tag{5}$$

where $x_t$is the position of maximum thickness on the airfoil, and t/c is the thickness to chord ratio. In all cases, the NACA 0015 airfoil is chosen as the standard airfoil wing with $t/c = 0.15$, and $x_t = 0.3c$. The form factor of the fuselage is given by:

$$FF_f = 1 + \frac{60}{(l_f/d_f)^3} + \frac{l_f/d_f}{400} \tag{6}$$

For all cases, the interference factor is assigned a value of 1 for simplicity. The induced drag is calculated as:

$$C_{Di} = \frac{C_L}{\pi eAR}, \tag{7}$$

where e is the Oswald factor. The miscellaneous drag is conservatively assumed to be 20 % of the wing drag. Once all the individual contributors are estimated, they are summed to give the total drag.

C. Thrust Model

To appropriately size the motors and propellers, the thrust and torque required for different stages of the flight mission must be considered. For the current tilt rotor configuration, the motor-propeller combination must to be able to provide the necessary thrust and torque required during each of hover, climb, cruise and banking. In order to calculate the requisite propeller diameters and motor RPM, a Blade Element Momentum (BEM) model is implemented in the optimization routine.

The BEM model divides each propeller blade into individual sections and calculates the local flow velocities and angles of attack by considering the cruise speed, RPM and local radii of the individual sections. A Clark Y airfoil is considered as the blade airfoil for all the cases. All hubs are assumed to have a constant radius of 0.3 m and the propeller blades are divided into 30 elements for the BEM calculations. By integrating the lift and drag of each individual section with the appropriate trigonometric identities, the total thrust, torque and power generated by each blade is calculated. The induced flow angle at each section is accounted for and estimated by using an iterative Newtons-Raphson's method. Additionally, Prandtl's tip and hub corrections are applied. A constraint is placed to restrict the blade tip Mach number to 0.85. To ensure the blade does not stall at any section, the allowable angle of attack range at each section is constrained between -4 and 13 °.

Previous studies indicated the relatively large contribution to total empty weight by the motors (e.g. [8]). Additionally, using the weight model for the motor provided in Appendix A, it can be seen that the motor weight is driven by required torque. Thus, for the sake of the optimization, it was decided that the flight mode that produced the largest requirements for torque would be chosen as the limiting factor in motor selection. For tilt rotors, the motor and propeller must be designed to be efficient in vastly different operating conditions- hover, cruise, climb and bank. In particular, the freestream velocities experienced by the propellers in hover are naturally significantly lower than experienced in climb, cruise or bank. It has been established that larger blade twist angles are required for an efficient cruise propeller as opposed to an efficient hover propeller [14]. Thus, designing a propeller efficient at all flight conditions is a separate optimization in itself. For the present study, it is assumed that a collective pitch can be applied to the blades, where at hover, the blades would all assume a lower collective pitch then switch to a higher pitch for the other flight modes. A constant twist is assumed on the blade with the root set at 70° and the tip at 20°. First, the thrust required at each flight condition is considered, and the BEM model is applied to determine the corresponding torque.

Thrust produced by the motor-propeller combination at hover should be able to counter the weight of the aircraft. An additional factor can be considered to account for maneuvarability. To determine the thrust required during phases of flight other than hover, a constraint analysis was performed. Constraint analysis is used to assess the relative

significance of performance constraints on the design. In the present case, for each operating condition, the thrust to weight ratio (T/W) is related to the wing loading (W/S). The graph is then read by noting that any combinations of W/S and T/W that are above the constraint curves will result in a design that meets those requirements. In the present study, minimum performance criteria are applied for each configuration, irrespective of the payload and range. Specifically, two conditions are imposed: one for banking, and one for climbing. The plane must be able to sustain a constant velocity turn for an assumed cruise speed of 60 m/s, while banking at an angle of 60 ° to the horizontal at its cruise altitude. Additionally, the plane must be able to climb at a rate of 3 m/s at 75 % of its cruising velocity. Considering these two conditions, the thrust to weight ratios can be expressed as follows:

$$T/W_{bank} = q(\frac{C_{Dmin}}{(W/S)} + k(\frac{n}{q})^2(W/S)) \tag{8}$$

$$T/W_{cruise} = V_v/V + \frac{q}{W/S}C_{Dmin} + \frac{k}{q}W/S \tag{9}$$

Here, q is the dynamic pressure, C_{Dmin} is the minimum drag coefficient , for both cases assumed to be 0.04 in accordance with planes of similar class [10], k is the lift induced drag constant calculated by using an aspect ratio of 12, $n = 1/cos(\phi)$ is the load factor with ϕ being the bank angle, and V_v is the vertical velocity. The graphs for both conditions are shown in figure 3 with the red dotted lines representing the limits of T/W used in the optimization based on a general range of T/W used in actual aircraft [8]. It can be seen that in the concerned range, thrust requirements for banking are generally higher than the requirements for climbing. Thus, the bank condition was chosen for implementation into the optimization. It must be noted that the thrust requirements for cruise are simply the drag experienced at cruise and this will always be lower than banking thrust requirements. It is thus not considered here.

To compare the corresponding torque required in banking versus hover, a trial BEM calculation is applied considering a plane of $GW = 3,000kg$, based on the highest expected weight after optimization, and a T/W ratio of 0.16, based roughly on the mean T/W found between the limits in figure 3. Additionally, a three blade propeller configuration with a constant propeller diameter of 1.5 m is assumed. The cruise velocity is assumed to be 60 m/s. Two conditions are compared: hover and banking. For hover, the thrust required is calculated as $GW * g$, where g is the acceleration due to gravity. Based on these assumptions, each individual motor would be required to produce a thrust of around 4,720 N for banking, and 29,430 N for hover. Based on these values, divided by the number of motors (6), yield the individual thrust requirements for each motor-propeller combination. Results from the BEM calculation indicate that despite the hover condition thrust requirements being significantly higher than in banking, the torque requirements are in fact lower. Specifically, the banking configuration torque is estimated as 670 Nm, while the hover is estimated to be 417 Nm. The

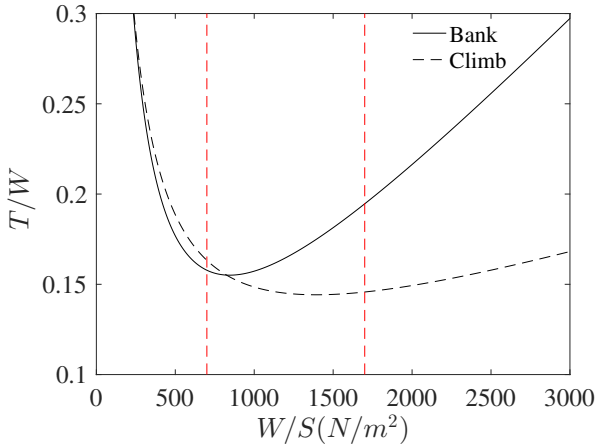

Fig. 3 Constraint diagram for bank and climb conditions.

difference in torque requirements for both conditions can be attributed to the difference in the collective pitch required for efficient operation in bank versus hover, where banking requires larger twist angles. While this specific calculation is not necessarily representative of the complete operating condition space, it is merely used as a reference for the motor selection. A more comprehensive optimization would ideally consider a wider range of limiting operating conditions. Thus, for the remainder of the optimization, only the banking condition is used to size the motor-propeller combination.

III. Optimization model

A constrained genetic algorithm was implemented for the optimization in MATLAB v16. Four parameters are chosen for the optimization- wing loading (W/S), cruise speed (U_{cr}), propeller diameter (D), and propeller RPM. A flowchart describing the optimization is shown in figure 4 .The routine starts with setting the payload and range. Global variables defined include the aspect ratio and number of rotors. An initial population size of 200 is used, where the population size was determined based on a convergence study. For subsequent generations, a crossover fraction of 0.65 is used, with a 5 % limit on the number of individuals guaranteed to survive the next generation. The constraint tolerance and penalty factor are set to 10^{-5} and 150 respectively. All runs converged within six generations. An initial gross weight estimate is provided. The parameters are then passed to the objective function and constraints. The constraint function calls the propeller module and ensures that the thrust output for each propeller diameter and RPM combination is within 100 N of the thrust requirements as estimated from the constraint analysis for banking. The tolerance for thrust was provided to account for the sensitivity of thrust to the propeller parameters. Subsequently, the objective function uses the parameters that satisfy the constraints to estimate the total drag of the aircraft followed by the empty weight estimates. The battery weight is then calculated and finally the gross weight, which has to be minimized, is calculated as the sum of the payload, empty weight and battery weight.

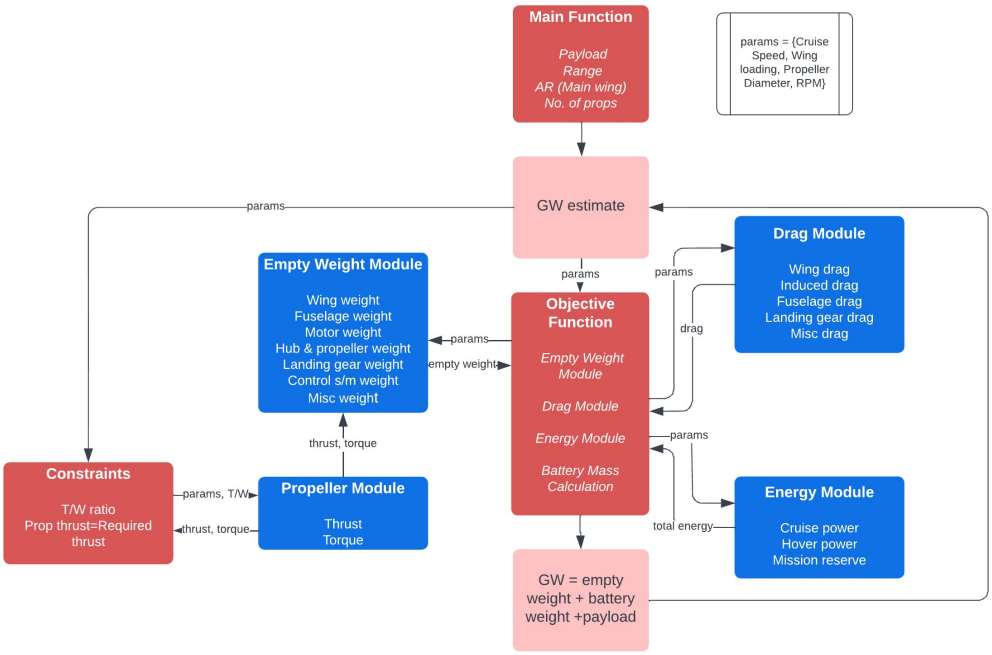

Fig. 4 Optimization code flowchart.

IV. Results

The resultant gross weights for different payloads and ranges are summarised in figure 5. For each payload and range combination approximately 4 runs were conducted. Here, the average of the optimization runs are plotted with variation between the results within a range of ±2.5%. The average values of L/D, disk loading, and empty weight fraction across all runs were found to be 17, 2,010 N/m^2 and 0.51 respectively.

The gross weight results show some interesting trends. As expected, gross weight is found to correlate to the range and the payload individually. For the same range and different payloads, the gross weight falls close to a linear fit. For 250 km, the fit can be described by equation $3.5x + 684$, where x is the payload weight in kilograms. Similarly, the equation for 150 km is $3.18x + 377$, and for 50 km it is $2.67x + 301$.

Figures 6, 7 and 8 show the individual component contribution to the total gross weight. Specific cases are chosen to highlight trends. It can be seen from the weight breakdown that increasing the payload results in a relatively consistent weight increase of all components, with the percentage contribution across all components remaining similar (figure 7). On the other hand, for the same payload, as the range is extended the major contributor to the increasing gross weight is the battery weight (figure 8). This is unsurprising, as longer ranges require larger energy spending with the same payload, resulting in larger batteries. This also points to a fact that it might be easier to design a scalable range aircraft than a scalable payload one.

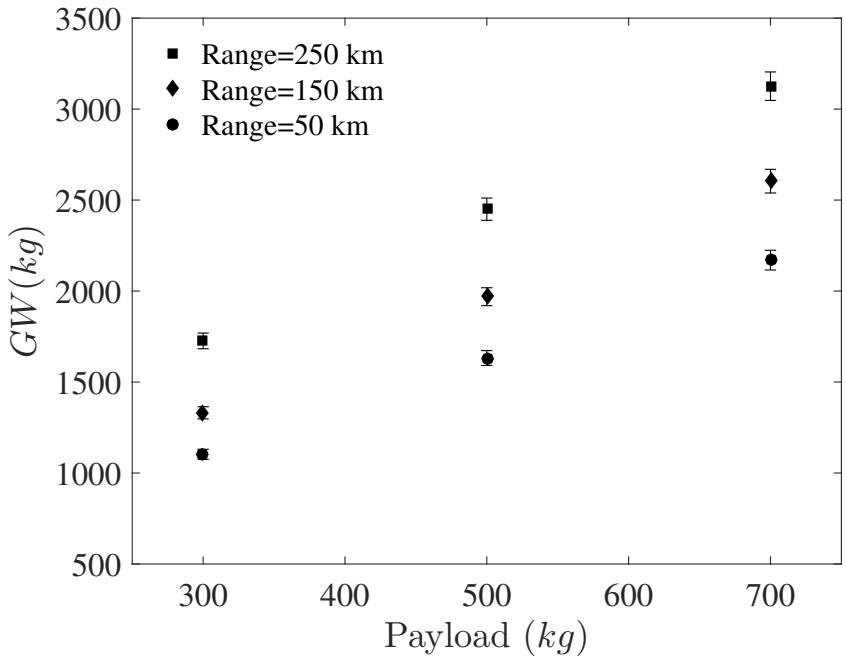

Fig. 5 Final results of optimization for the various ranges and payloads considered.

The two major contributors to the empty weight are the motors and the wings which together contribute to anywhere between 30 % and 40 % of the total aircraft empty weight (components+battery). The optimization thus attempts to proceed in a direction such as to minimize the contribution from these two sources. However, since the optimization considers a constraint analysis to estimate thrust requirements, it turns out that the motor weight and wing weight tend to drive the optimization in different directions. Figure 9 shows the contour of thrust to weight ratio as a function of the wing loading and cruise speed. The right plot shows the plot for a constant cruise speed. Ideally, minimization of the motor weight would drive the optimization towards the lowest thrust (and by extension, torque) possible that satisfies the constraint diagram. From the constraint diagram, lower T/W ratios correlate with lower wing loading within the current bounds considered. On the other hand, minimization of the wing weight drives the optimization towards higher values of wing loading, where a higher wing loading results in a wing wither lower area and hence, lower weight. These two opposing tendencies drive the optimization. The program then selects values of the parameters that minimize the sum of these two weights. From figure 9 it can be seen that cruise speeds between approximately 55-65 m/s offer the possibilities of lower thrust to weight ratio requirements while still maintaining a relatively high wing loading. The scatter of final optimized parameter values shown in figure 10 also confirms this trend where the mean of the cruise speeds is 60 m/s and the mean of the wing loading is 1,183 N/m^2.

The thrust requirements from the constraint diagram allow for multiple solutions for propeller diameter and RPM that

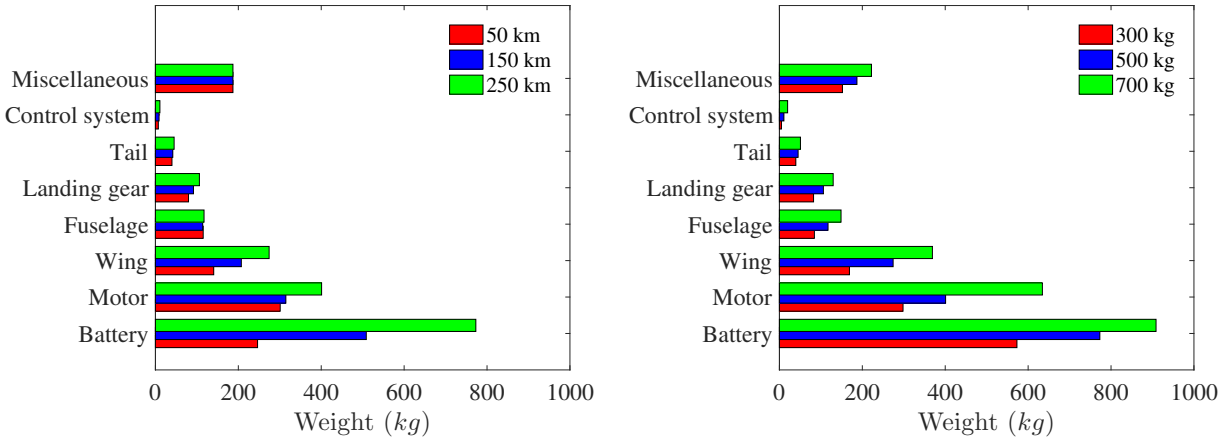

(a) **(b)**

Fig. 6 Individual component weight breakdown for (a) 500 kg payload and different ranges, and (b) 250 km range and different payloads.

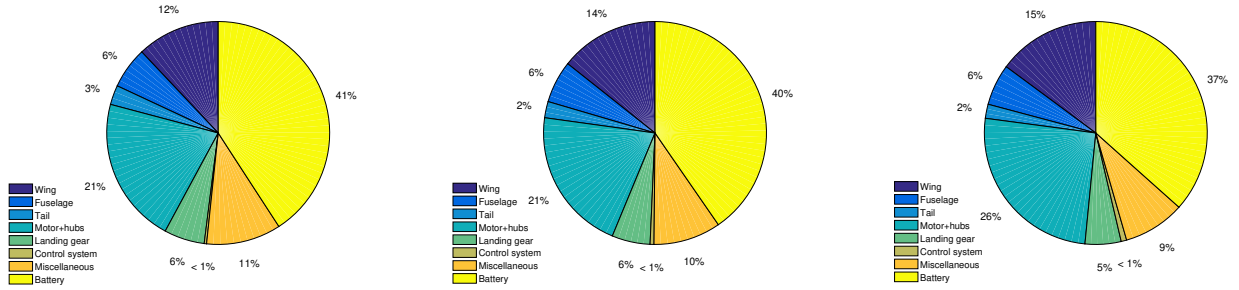

(a) **(b)** **(c)**

Fig. 7 Contribution of individual weights for 250 km range and payloads of (a) 300 kg (b) 500 kg and (c) 700 kg.

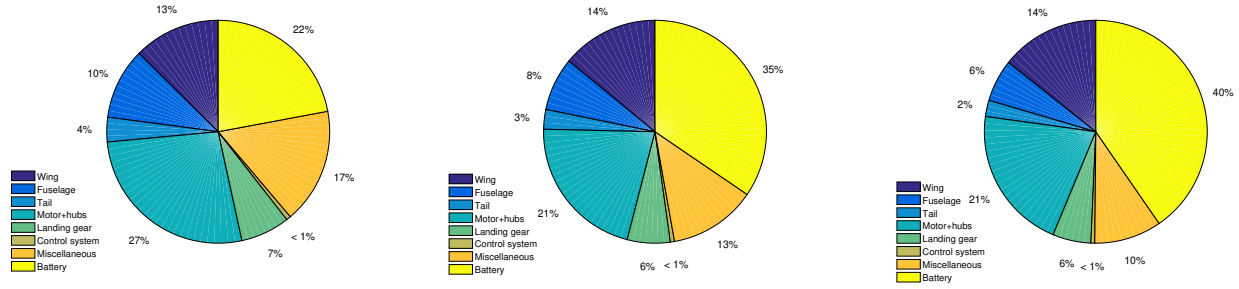

(a) **(b)** **(c)**

Fig. 8 Contribution of individual weights for 500 kg payload and ranges of (a) 50 km (b) 150 km and (c) 250 km

satisfy the thrust constraint and tolerance. Figure 10 shows that the optimization is generally driven towards lower propeller diameters with the mean diameter 1.56 m. Addition of noise constraints in the current optimization would presumably drive the propeller diameters higher along with lower RPM's.

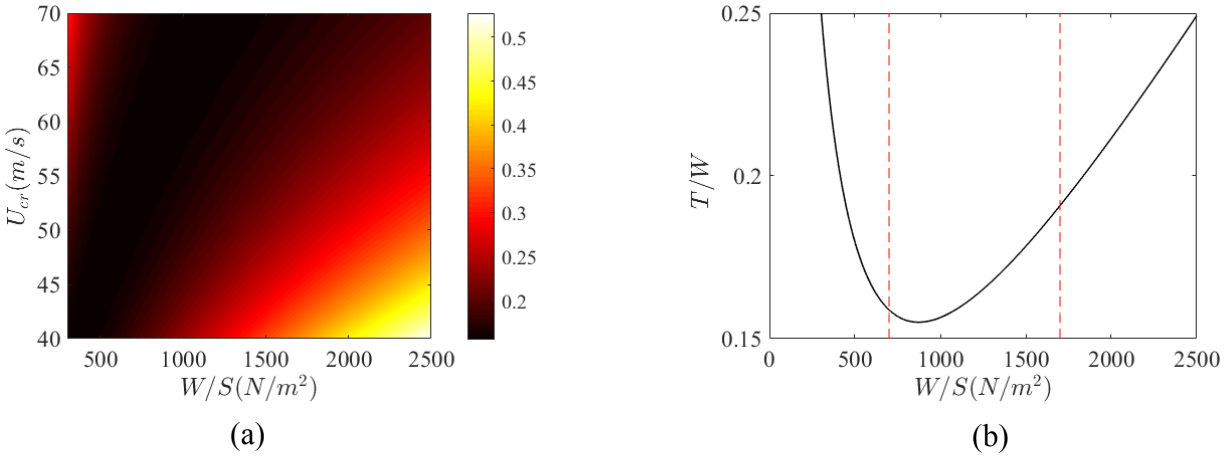

Fig. 9 (a) Contour plot of thrust to weight ratio as a function of wing loading and cruise speed. (b) Wing loading vs thrust to weight ratio at a fixed speed of U_{cr}=60 m/s.

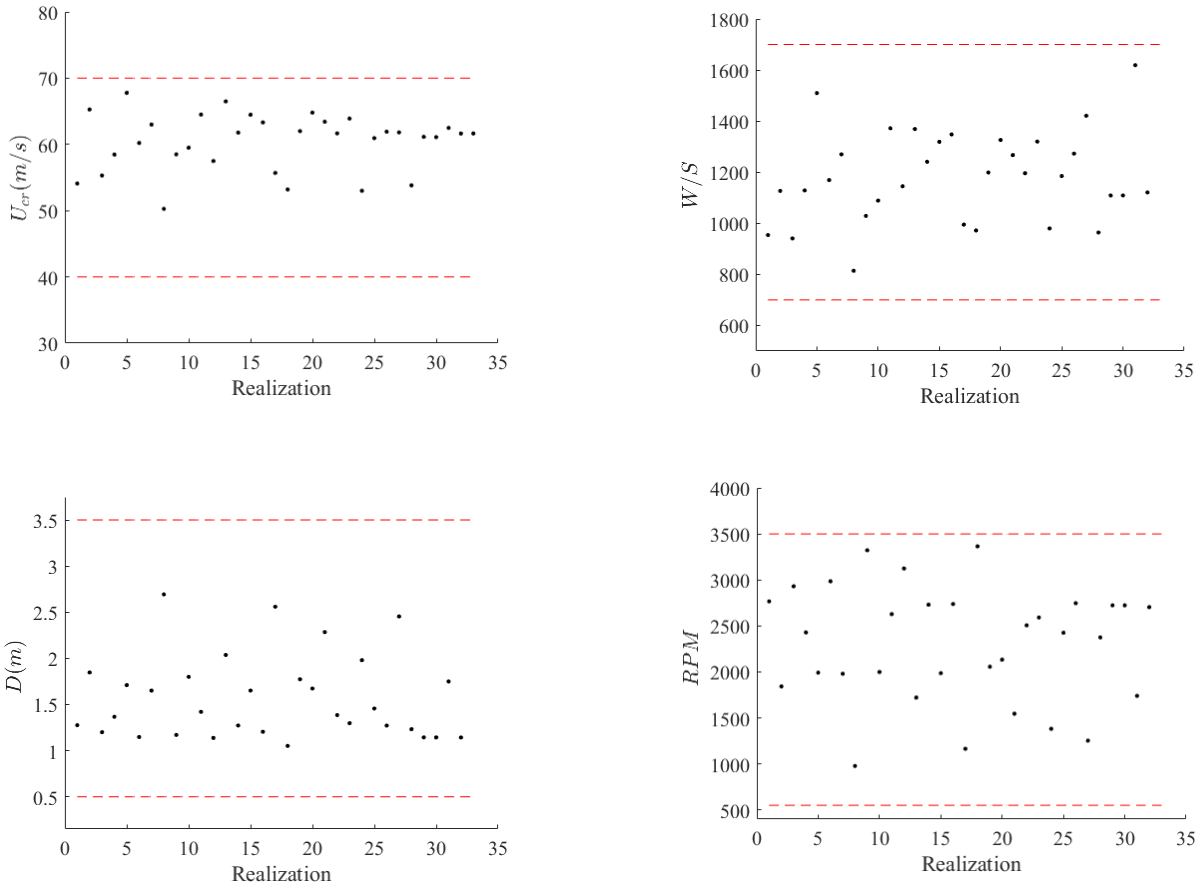

Fig. 10 Scatter of final parameters for the different realizations.

Table 4 shows the results of a few optimization runs for 300 kg payload. It can be seen that similar gross weight results are obtained with widely varying propeller diameters and wing loading. As an example, we can see that in Run

#7 has a propeller diameter of 1.148 m with cruise RPM of 2,985, whereas for Run #9 it is 2.694 m with RPM of 978. It is evident that the propeller diameter and RPM are inversely proportional as the code is trying to minimize the motor torque which is the basis for motor weight. Results for optimization runs for 500 kg and 700 kg payloads are shown in Appendix B. As such, a purely physics based optimization will result in multiple nearly optimal solutions. Further optimization is out of the scope of the present paper, however the solution set can be narrowed down further based on trade-off of noise, cost, recharging constraints and take-off/landing infrastructure related geometrical constraints .

The real-world validation of these results is difficult since no fully certified eVTOL tilt-rotor of such a configuration exists. However, the closest to certification is the Joby S4 which has payload of 455 kg (1 pilot plus 4 passengers, each with estimated weight of 91 kg), range of 240 km and a published aircraft weight of 1,755 kg [15]. Adding together the aircraft weight and payload gives a gross weight of 2,210 kg for Joby S4. Another source [16] shows the claim for maximum take-off weight as 2,177 kg for the same aircraft. This is comparable to the 2,275 kg obtained from present optimization using linear interpolation of results in figure 5, with the difference between 3% to 5%. It is important to note that there are some key differences between the two configurations. The pack level energy density claimed by Joby is 235 Wh/kg and their cruise speed is much higher than limits set in this paper. Furthermore, their assumptions for reserves are not clearly known. On the other hand, the empirical weight formulae used in this paper do not consider the latest technological advances in material science and structural design methodologies, which may offset the higher battery energy density assumption. Finally, the propulsion system also varies with Joby S4 having 5-bladed propellers whereas 3-bladed propellers are considered in present study. For the above reasons, this comparison only gives us initial confidence in the presented methodology, in absence of other information. As this study is expanded to include other configurations and more data is published by eVTOL developers, a more rigorous validation can be performed.

Table 4 Results for 300 kg payload

Run #	Range, km	GW, kg	Cruise Speed, m/s	W/S, N/m^2	D, m	RPM
1	50	1102	61.10	1109	1.143	2724
2	50	1114	62.50	1619	1.750	1740
3	50	1099	61.65	1121	1.143	2704
4	150	1374	63.32	1348	1.204	2738
5	150	1312	53.00	980	1.981	1382
6	150	1306	53.82	964	1.233	2375
7	250	1736	60.21	1169	1.148	2985
8	250	1702	63.00	1270	1.651	1980
9	250	1740	50.28	814	2.694	978

V. Conclusions

A methodology for eVTOL aircraft sizing is presented that focuses on integrating performance parameters such as banking and climb requirements at the early stages of design process along with the conventional parameters such as payload, range, wing loading, propeller diameter and propeller RPM. By incorporating the performance criteria through the use of a constraint diagram, the thrust and torque required during different phases of flight can be used to satisfactorily size the motor-propeller combination. Additionally, the thrust obtained from the constraint diagram is related to the wing loading through first principles. The present optimization uses a genetic algorithm with the objective function of minimizing gross weight. It is applied to a tilt-rotor configuration in order to size the eVTOL for UAM (50, 150 km) and RAM (250 km) missions with varying payloads. The gross weight obtained from this methodology is within 3-5 % of the published weight of the only aircraft in a similar class that is close to certification.

The key outcomes from the study can be summarised as follows:

- The inclusion of constraints diagram for banking requirement in cruise along with the motor-out condition for safety drives the motor sizing. The motor is sized for maximum torque, and ideally should consider the flight mode that requires the highest torque in addition to the redundancy offered by a motor-out condition.
- It is found that for the same range and different payloads, the gross weight falls close to a linear fit. Increasing the payload results in a relatively consistent weight increase of all components. Whereas, for the same payload, as the range is extended, the major contributor to higher gross weight increase is the battery weight. Thus, scaling an aircraft by increasing the payload is potentially more technologically challenging compared to simply scaling an aircraft based on range, where the battery requirements will primarily drive the design.
- The two major contributors to the empty weight are the motors and the wings. The optimization thus generally proceeds in the direction where the total contribution of these two weights is minimal.
- The lowest gross weight for a given payload and range combination can potentially be met by multiple solutions that may vary significantly in rotor diameter and wing loading. Further optimization of concepts would require incorporating considerations for noise, cost, supply chain and manufacturability, amongst others.

The next steps should include validating this methodology for other eVTOL configurations and comparison of the results with real-world data. In the absence of certified aircraft, details of sub-scale models could be used for validation.

Acknowledgments

References

[1] Polaczyk, N., Trombino, E., Wei, P., and Mitici, M., "A review of current technology and research in urban on-demand air mobility applications," *8th Biennial Autonomous VTOL Technical Meeting and 6th Annual Electric VTOL Symposium*, 2019, pp. 333–343.

[2] Brown, A., and Harris, W., "A vehicle design and optimization model for on-demand aviation," *2018 AIAA/ASCE/AHS/ASC Structures, Structural Dynamics, and Materials Conference*, 2018, p. 0105.

[3] Bacchini, A., and Cestino, E., "Electric VTOL configurations comparison," *Aerospace*, Vol. 6, No. 3, 2019, p. 26.

[4] Nathen, P., Strohmayer, A., Miller, R., Grimshaw, S., and Taylor, J., "Architectural performance assessment of an electric vertical take-off and landing (e-VTOL) aircraft based on a ducted vectored thrust concept," , 2021.

[5] Palaia, G., Abu Salem, K., Cipolla, V., Binante, V., and Zanetti, D., "A Conceptual Design Methodology for e-VTOL Aircraft for Urban Air Mobility," *Applied Sciences*, Vol. 11, No. 22, 2021, p. 10815.

[6] Hascaryo, R. W., and Merret, J. M., "Configuration-Independent Initial Sizing Method for UAM/eVTOL Vehicles," *AIAA AVIATION 2020 FORUM*, 2020, p. 2630.

[7] Higgins, R. J., Barakos, G. N., Shahpar, S., and Tristanto, I., "A computational fluid dynamic acoustic investigation of a tiltwing eVTOL concept aircraft," *Aerospace Science and Technology*, Vol. 111, 2021, p. 106571.

[8] Kadhiresan, A. R., and Duffy, M. J., "Conceptual design and mission analysis for eVTOL urban air mobility flight vehicle configurations," *AIAA Aviation 2019 Forum*, 2019, p. 2873.

[9] Lee, B.-S., Tullu, A., and Hwang, H.-Y., "Optimal design and design parameter sensitivity analyses of an eVTOL PAV in the conceptual design phase," *Applied Sciences*, Vol. 10, No. 15, 2020, p. 5112.

[10] Gudmundsson, S., *General aviation aircraft design: Applied Methods and Procedures*, Butterworth-Heinemann, 2013.

[11] Datta, A., Elbers, S., Wakayama, S., Alonso, J., Botero, E., Carter, C., and Martins, F., "Commercial intra-city on-demand electric-VTOL status of technology," *NASA Aeronautics Research Institute, Technical Report TVF WG*, Vol. 2, 2018.

[12] Raymer, D., *Aircraft design: a conceptual approach*, American Institute of Aeronautics and Astronautics, Inc., 2012.

[13] Smart, J. T., and Alonso, J. J., "Primary Weight Estimation for eVTOLs via Explicit Analysis and Surrogate Regression," *AIAA Aviation 2019 Forum*, 2019, p. 3679.

[14] Leishman, J. G., and Rosen, K. M., "Challenges in the Aerodynamic Optimization of High-Efficiency Proprotors," *Journal of the American Helicopter Society*, Vol. 56, No. 1, 2011, pp. 12004–12004.

[15] Joby Aviation, "Joby Analyst Day presentation," https://d1io3yog0oux5.cloudfront.net/_086372 0ccf49e83240a9a2d5a54a85c8/jobyaviation/db/1086/9729/pdf/Joby+Aviation_Analyst+Day+Presentation.pdf, 2021. [Online; accessed 22-May-2022].

[16] Jeremy Bogaisky, "Has Joby Cracked The Power Problem To Make Electric Air Taxis Work?" https://www.forbes.com/sites/jeremybogaisky/2020/11/23/joby-batteries-electric-aviation/?sh=609508ea76a7, 2020. [Online; accessed 22-May-2022].

A. Appendix - Weights Formulae

This Appendix presents the formulae used for weight estimation and their respective sources.

The weight estimates for structural components were made using empirical equations from Raymer [12] that are derived from historical general aviation aircraft. Units are as per original source.

$$W_{Wing} = 0.036 S_w^{0.758} W_{fw}^{0.0035} \left(\frac{A}{cos^2\Lambda}\right)^{0.6} q^{0.006} \lambda^{0.04} \left(\frac{100t/c}{cos\Lambda}\right)^{-0.3} (N_z W_{dg})^{0.49} \tag{10}$$

$$W_{Fuselage} = 0.052 S_f^{1.086} (N_z W_{dg})^{0.177} L_t^{-0.051} (L/D)^{-0.072} q^{0.241} + W_{press} \tag{11}$$

$$W_{Ht} = 0.016 (N_z W_{dg})^{0.414} q^{0.168} S_{ht}^{0.896} (\frac{100t/c}{cos\Lambda})^{-0.12} (\frac{A}{cos^2\Lambda_{ht}})^{0.043} \lambda_h t^{-0.02} \tag{12}$$

$$W_{Vt} = 0.073(1 + 0.2(H_t/H_v))(N_z W_{dg})^{0.376} q^{0.122} S_{vt}^{0.873} (\frac{100t/c}{cos\Lambda_{vt}})^{-0.49} (\frac{A}{cos^2\Lambda_{vt}})^{0.357} \lambda_{vt}^{0.039} \tag{13}$$

$$W_{MainLandingGear} = 0.095 (N_l W_l)^{0.768} (\frac{L_m}{12})^{0.409} \tag{14}$$

$$W_{NoseLandingGear} = 0.125 (N_l W_l)^{0.566} (\frac{L_n}{12})^{0.845} \tag{15}$$

$$W_{FlightControlSystem} = 0.053 L^{1.536} B_w^{0.371} (N_z W_{dg} * 10^{-4})^{0.08} \tag{16}$$

The powertrain component weights are estimated using following formulae presented by Kadhiseran et al [8]

$$W_{PropHubs} = \frac{2.20462}{1000} * (\frac{7200}{500} * (T_{rotor} * 4.4482 - 300) + 800) * n_{rotors} \tag{17}$$

$$W_{Motors} = 2.20462 * (\frac{58}{990} * (\tau * 1.3558 - 10) + 2) * (n_{rotors}) \tag{18}$$

$$W_{MotorController} = 2.20462 * (\frac{49.9}{398} * (P_{motor} - 2) + 0.1) * (n_{rotors}) \tag{19}$$

The following aircraft equipment and accessory weights were derived from information presented by J.Smart [13]

$$W_{Avionics} = 20 \tag{20}$$

$$W_{Seats} = 17.5 * (n_{passengers} + n_{crew}) \tag{21}$$

$$W_{PitchServo} = 0.75 * n_{rotors} \tag{22}$$

$$W_{TiltMechanism} = 7.5 * n_{rotors} \tag{23}$$

$$W_{ECS} = 7.5 \tag{24}$$

$$W_{BRS} = 22.5 \tag{25}$$

Terminology for Appendix A

W_{Wing}	=	Weight of the wing, lb
S_w	=	Trapezoidal wing area, ft^2
W_{fw}	=	Weight of fuel in wing, lb
A	=	Aspect Ratio
Λ	=	Wing sweep at 25% MAC
q	=	Dynamic pressure at cruise, lb/ft^2
λ	=	Wing taper ratio
$W_{Fuselage}$	=	Weight of fuselage,lb
S_f	=	Fuselage wetted area, ft^2
N_z	=	Ultimate load factor; 1.5*limit load factor
W_{dg}	=	Design gross weight, lb
L_t	=	tail length; wing quarter-MAC to tail quarter-MAC, ft
L	=	Fuselage structural length, ft (excludes radomes, tail cap)
D	=	Fuselage Structural depth, ft
W_{press}	=	Weight penalty due to pressurization, lb
W_{Ht}	=	Weight of horizontal tail(HT), lb
S_{ht}	=	Wetted surface area of HT, lb
Λ_{ht}	=	Wing sweep of HT at 25% MAC

λ_{ht} = HT taper ratio

$\frac{H_t}{H_v}$ = 0.0 for conventional tail; 1.0 for T-tail

W_{Vt} = Weight of Vertical Tail(VT), lb

S_{vt} = Wetted surface area of VT, lb

Λ_{vt} = Wing sweep of VT at 25% MAC

λ_{vt} = VT taper ratio

$W_{MainLandingGear}$ = Weight of main landing gear, lb

N_l = Ultimate landing load factor (typically, =$N_{gear} * 1.5$

W_l = Landing design gross weight, lb

L_m = Length of main landing gear, lb

L_n = Length of nose landing gear, lb

$W_{NoseLandingGear}$ = Weight of nose landing gear, lb

$W_{FlightControlSystem}$ = Weight of flight control systems

B_w = Wing span, ft

$W_{PropHubs}$ = Weight of propellers and hubs, lb

T_{rotor} = Thrust per rotor, N

n_{rotors} = Number of rotors

W_{Motors} = Weight of motors, lb

τ = Motor torque, N.m

$W_{MotorController}$ = Weight of motor controller, lb

P_{motor} = Motor power, kW

$W_{Avionics}$ = Weight of avionics, kg

W_{Seats} = Weight of seats, kg

$n_{passengers}$ = Number of passengers

n_{crew} = Number of crew

$W_{PitchServo}$ = Weight of pitch servos, kg

$W_{TiltMechanism}$ = Weight of tilt motors, kg

W_{ECS} = Weight of Environmental Control System, kg

W_{BRS} = Weight of Ballistic Recovery System, kg

B. Appendix - Details of 700 kg and 500 kg optimization runs

Table 5 Results for 500 kg payload

Run #	Range, km	GW, kg	Cruise Speed, m/s	W/S, N/m^2	D, m	RPM
1	50	1608	64.48	1319	1.651	1987
2	50	1614	63.90	1320	1.298	2592
3	50	1675	61.81	1421	2.455	1254
4	150	1936	58.46	1129	1.367	2429
5	150	1971	61.78	1241	1.272	2731
6	150	1974	61.92	1273	1.272	2747
7	250	2468	55.30	941	1.200	2931
8	250	2474	66.50	1369	2.037	1721
9	250	2439	64.80	1326	1.673	2133

Table 6 Results for 700 kg payload

Run #	Range, km	GW, kg	Cruise Speed, m/s	W/S, N/m^2	D, m	RPM
1	50	2151	65.27	1127	1.848	1842
2	50	2176	57.50	1145	1.138	3124
3	50	2228	53.20	972	1.051	3365
4	150	2597	54.10	954	1.276	2767
5	150	2583	64.50	1372	1.420	2628
6	150	2632	55.70	995	2.560	1165
7	250	3087	58.50	1029	1.170	3322
8	250	3109	59.50	1089	1.800	1999
9	250	3185	63.43	1267	2.285	1546